The threshold of coexistence and critical behaviour of a predator–prey cellular automaton

The threshold of coexistence and critical behaviour of a predator–prey cellular automaton

Everaldo Arashiro and Tânia Tomé

Instituto de Física, Universidade de São Paulo, Caixa postal 66318,
05315-970 São Paulo, SP, Brazil

Abstract
We study a probabilistic cellular automaton to describe two population biology problems: the threshold of species coexistence in a predator–prey system and the spreading of an epidemic in a population. By carrying out mean-field approximations and numerical simulations we obtain the phase boundaries (thresholds) related to the transition between an active state, where prey and predators present a stable coexistence, and a prey absorbing state. The numerical estimates for the critical exponents show that the transition belongs to the directed percolation universality class. In the limit where the cellular automaton maps into a model for the spreading of an epidemic with immunization we observe a crossover from directed percolation class to the dynamic percolation class. Patterns of growing clusters related to species coexistence and spreading of epidemic are shown and discussed.

PACS numbers: 05.70.Ln, 87.23.Cc, 64.60.Ht

(Some figures in this article are in colour only in the electronic version)

1. Introduction

In 1958, Huffaker [1], in a pioneering experiment, was able to maintain in the laboratory a population of prey and predators coexisting and presenting self-sustained coupled time oscillations. He has verified that persistence of species was only possible in a large and heterogeneous space. Since then different models have been proposed to explain the role of space in determining the species coexistence [2–13]. A common feature of these models is that they are based either on interacting particle systems [14], also called stochastic lattice models [4], or on probabilistic cellular automata. These descriptions are appropriate and relevant when considering predator–prey systems which are under conditions of very low species population densities and/or when their habitat is spatially heterogeneous [2].

In the present paper we study a stochastic model that takes into account the spatial structure explicitly to describe two population biology issues: the threshold of species coexistence in a predator–prey system and the spreading of an infectious disease in a population. The dynamics associated with the systems is a Markovian discrete time process, namely a probabilistic cellular automaton. The individuals of each population are treated as discrete and they are supposed to occupy the sites of a two-dimensional lattice. Birth and death of individuals are included in the stochastic rules which take into account the limited resources for proliferation and local interactions. We consider that one prey individual can be born in an empty site if there are prey in the neighbourhood of the empty site; predators eat prey if they are in the first neighbourhood of a site occupied by prey; predators die spontaneously. Each process occurs according to a probability and the proliferation of prey and the predation are mimicked by processes which are similar to the catalytic creation process in the contact model [14].

By performing a simple mean-field analysis of this automaton, we derive time evolution equations for the densities; these can be compared to those provided by an unstructured metapopulation dynamics approach equations [15, 16] for the fractions of empty patches, patches colonized by prey and patches colonized by predators. Thus, at a simple mean-field level, the time evolution equations for the densities of prey and predators can be mapped into an extended version of Lotka–Volterra equations [17, 18], which contains a logistic term [15]. The simple mean-field approach shows that the system evolves in time and eventually reaches stationary states that can be either active states, where prey and predators have a stable coexistence, or absorbing states. There is thus a transition from the stable coexistence state to a state where predators have been extinct.

To analyse the relation between the spatial distribution of species and persistence and to find the thresholds of coexistence we carry out numerical simulations. A particularly useful numerical method for models with absorbing states, is the so-called time-dependent simulation (or spreading analysis) [19–33]. This method allows us to obtain the phase boundaries together with the critical exponents. The scaling analysis of the time-dependent simulation yields a set of dynamic critical exponents and thus the possibility of classification of models in universality classes. Here, we have found that the automaton exhibits a line of continuous phase transition which belongs to the universality class of directed percolation, for all sets of parameters such that the prey birth probability is different from zero. When this probability vanishes there occurs a crossover to the universality class of dynamic isotropic percolation.

The automaton, in the above-mentioned limit, can be mapped into a model for the spreading of an epidemic with immunization, a general epidemic process [15, 20, 21, 34, 35]. This mapping can be accomplished by making the correspondence: prey and predators individuals with susceptible and infected individuals, respectively. This is in accordance with a modelling of infectious diseases by considering slight variations of the Lotka–Volterra predator–prey equations [36]. The spreading of an epidemic can also be interpreted as a limiting case of the forest fire with immunization automaton introduced by Drossel and Schwabl [37]. Our automaton presents similarities with the Drossel and Schwabl automaton, which will be exploited later.

This paper is organized as follows. In section 2 we describe the predator–prey cellular automaton, a mean-field approach and time-dependent simulation. Critical properties and pictures of growing clusters generated by the simulations are shown in the same section. In section 3 we analyse the spreading of an epidemics with immunization. We briefly summarize our results in section 4.

2. Predator–prey probabilistic cellular automaton

2.1. The model

We assume that each individual of each species population can reside on the sites of a regular square lattice which represents their habitat. A site in the lattice can be in one of three states: occupied by a prey individual (X); occupied by a predator individual (Y) or empty (Z). The predator–prey probabilistic cellular automaton comprehends the following processes:

$$Z + X \rightarrow 2X, \tag{1}$$

$$X + Y \rightarrow 2Y, \tag{2}$$

and

$$Y \rightarrow Z. \tag{3}$$

The transitions between states obey probabilistic rules which depend on the state of the given site and on the states of its four nearest neighbours at the north, east, south and west (which defines the neighbourhood). The update is synchronous and the rules are

  (i) a prey individual can be born in an empty site with a probability $a/4$ times the number of sites occupied by prey in the neighbourhood, process (1);
 (ii) a predator individual can be born in a site occupied by a prey if there are predators in its neighbourhood. Prey disappear instantaneously and give place to a new predator. The probability of this process is $b/4$ times the number of sites occupied by predators in the neighbourhood, process (2);
(iii) the death of predators is spontaneous: a site occupied by a predator can be evacuated with a probability c. This process reintegrates to the system the resources for prey proliferation, process (3).

The model has three parameters a, b and c, with $0 \leqslant a \leqslant 1$, $0 \leqslant b \leqslant 1$ and $0 \leqslant c \leqslant 1$. However, we assume that [4, 7] $a + b + c = 1$, thus just two parameters are independent. We consider the parametrization: $a = (1 - c)/2 - p$ and $b = (1 - c)/2 + p$. The parameter p is such that $-1/2 \leqslant p \leqslant 1/2$ and parameter c denotes the death probability of predators, $0 \leqslant c \leqslant 1$. This parametrization allows us to analyse the model in a triangular phase diagram $p - c$, as shown in figure 1.

The present automaton exhibits similarities with the forest fire automaton with immunity introduced by Drossel and Schwabl [37]. Let us call η_i a dynamic variable which takes the values $\eta_i = 0, 1$ or 2 according whether site i is empty, occupied by one *prey* individual (a *green tree* in the forest-fire model) or by one *predator* individual (a *burning tree* in the forest-fire model). The transitions between states in both models are cyclic $0 \rightarrow 1 \rightarrow 2 \rightarrow 0$. However, in the present model the transition $0 \rightarrow 1$ is catalytic whereas in the forest-fire model it is spontaneous. The transition $1 \rightarrow 2$ is catalytic in both models and the transition $2 \rightarrow 0$ is spontaneous in both models. The processes $0 \rightarrow 1$ and $1 \rightarrow 2$ occur with probabilities a and b, respectively, for the predator–prey automaton and p and $1 - g$ (g is called immunity), respectively, for the forest-fire model. The process $2 \rightarrow 0$ occurs with probability c in the predator–prey model and with probability 1 in the forest-fire model.

2.2. Dynamic mean-field approximation

The simplest theoretical description of the predator–prey probabilistic cellular automaton is given by the one-site dynamic mean-field approximation (also called simple mean-field
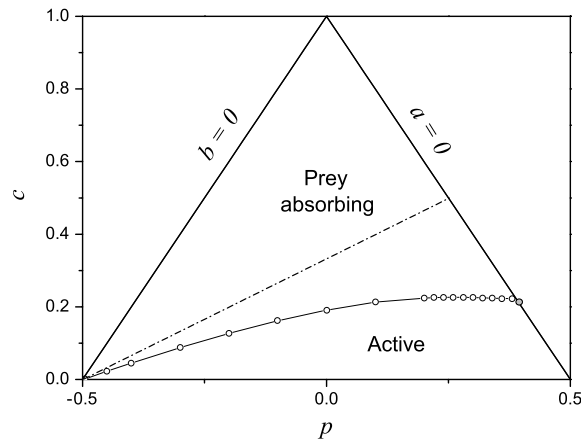
Figure 1. Phase diagram in the plane $p - c$, showing regions corresponding to the prey absorbing phase and the active phase. Phases are separated by a transition line obtained from mean-field approximation (dotted-dashed line) and time-dependent simulations (full line).

approximation) [38] where the probability of a cluster of sites is written as the product of the probabilities of each site. Under this approach we can derive the following two-dimensional map:

$$x_{\ell+1} = ax_\ell(1 - x_\ell - y_\ell) - bx_\ell y_\ell + x_\ell, \tag{4}$$

$$y_{l+1} = bx_\ell y_\ell + (1 - c)y_\ell, \tag{5}$$

where x_ℓ and y_ℓ are the mean number of prey and predator individuals per site at time ℓ, respectively. We remark that the density of empty sites z_ℓ is given by

$$z_\ell = 1 - x_\ell - y_\ell. \tag{6}$$

Equations (4) and (5) differ in an important feature from the Lotka–Volterra model, namely, the presence of the logistic term $z_\ell = 1 - x_\ell - y_\ell$ which means to say that amount of resources for prey proliferation is limited.

For $a \neq 0$, the stationary solutions of equations (4) and (5) are

$$(x_1, y_1) = (0, 0), \qquad (x_2, y_2) = (1, 0) \tag{7}$$

and

$$(x_3, y_3) = \left(\frac{c}{b}, \frac{1 - c/b}{1 + b/a} \right). \tag{8}$$

The two first solutions are trivial and correspond respectively to the absorbing state where both species have been extinct and the absorbing state where the space is completely full of prey. The third solution depends on the parameters a, b and c and is an active solution. Performing a linear analysis of stability we find that: the solution (x_1, y_1) is unstable for any set of the parameters; the solution (x_2, y_2), which corresponds to the prey absorbing state, is stable in the region $b \leqslant c$; and the active solution (x_3, y_3), where there is coexistence of species, is stable for $b > c$. So that, as shown in figure 1, a continuous transition line, described by $b = c$ or $c = (1 + 2p)/3$, crosses the entire phase diagram and separates the absorbing prey phase and the active phase, characterized by nonzero densities of prey and predators.
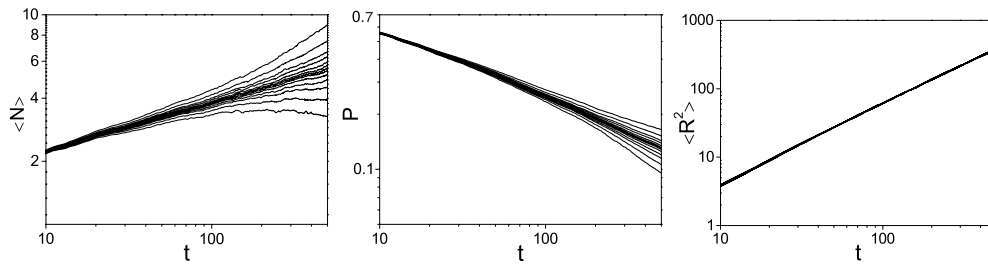
Figure 2. Log–log plot of the mean number of predators $\langle N \rangle$ (left panel), the survival probability P (middle panel) and the mean-square distance of spreading of predators $\langle R^2 \rangle$ (right panel), as a function of the time t, for $p = 0$. Each figure shows the behaviour of these quantities for different values of c. From top to bottom, in each figure, c is varied from 0.18875 until $c = 0.19275$ in different steps.

We may conclude that the simplest mean-field approximation for the predator–prey probabilistic cellular automaton is able to show, under a robust set of control parameters, that prey and predators can coexist without extinction. It is worth noticing again that the model, in this simple approximation, has an analogy with an unstructured metapopulation model with empty patches, patches colonized by prey and patches colonized by predators [15, 16].

2.3. Time-dependent simulation

To carry out a time-dependent simulation analysis for the predator–prey cellular automaton we follow the time evolution of states very close to the prey absorbing state. We depart from an initial condition ($t = 0$) with a single predator at the origin of a lattice covered by prey. Once the system is placed in the initial condition we apply the local rules (i), (ii) and (iii), described in section 2.1, and let it evolves in time. We have considered 10 000 samples (independent runs) all starting with this same condition. For each fixed value of p we vary c near its transition value. The simulations were performed in systems sufficiently large so that predators do not reach the borders of the lattice.

We have investigated the behaviour of the following quantities: the survival probability of predators P, that is, the probability that predators have not been extinct until time t; the mean number of predators $\langle N \rangle$ at time t, whose average is calculated over all the samples, including those where predators have been extinct before time t; and the average mean-square distance of spreading of predators from the origin, $\langle R^2 \rangle$. This average is calculated by taking into account only the samples that survived until time t. According to the scaling laws for time-dependent simulations [19], for large values of t, we expect, at the critical point, the following power laws,

$$\langle N \rangle \sim t^{\eta}, \qquad P \sim t^{-\delta}, \qquad \langle R^2 \rangle \sim t^{z}, \tag{9}$$

where η, δ and z are the critical exponents.

As can be seen in figure 2, the log–log plot of the mean number of predators, as well as of the survival probability, show very well-defined critical and off-critical asymptotic behaviours. Therefore, it is possible to obtain the phase boundaries together with the critical exponents. From figure 2 we get the following estimates for the critical exponents $\eta = 0.230(9)$, $\delta = 0.451(6)$, and $z = 1.134(4)$, for $p = 0$ (that is, for $a = b$). The same values of exponents, within the statistical errors, were found for distinct values of p along
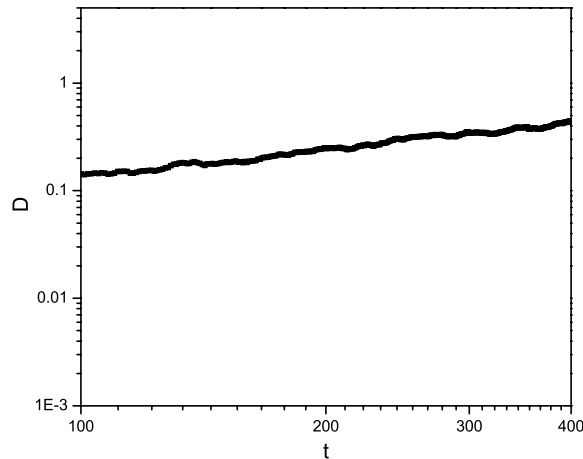
Figure 3. Logarithmic derivative D of $\langle N \rangle$ with respect to c. For $p = 0$ and considering values of c slightly above and below the critical value.

the critical line $c(p)$ (excluding the critical point for which $a = 0$). These values of the dynamic critical exponents are consistent with those of the directed percolation class in $(2+1)$ dimensions [29]. This dynamic critical behaviour has been obtained for a diversity of models with finite number of asymmetric absorbing states [26–31, 41, 42].

The critical exponent associated with the time correlation length $\nu_\parallel$ can be obtained from the time-dependent simulations. Here, the estimation was accomplished by studying the time behaviour of the derivative D of the mean value of predators $\langle N \rangle$. From the scaling laws it can be shown that [23],

$$D = \frac{d \log \langle N \rangle}{d \log c} \simeq t^{1/\nu_\parallel}, \tag{10}$$

at the critical value of c. In a simulation run the derivative was calculated considering finite differences; this procedure requires data for values of c slightly above and below the critical value. The behaviour of D, for $p = 0$, is shown in figure 3, from which we obtained the exponent $\nu_\parallel = 1.29(10)$, in agreement with the estimated value $\nu_\parallel = 1.295(6)$ [29] for the directed percolation in $(2 + 1)$ dimensions.

In figure 1 it is shown that the transition line $c(p)$ is determined from our time-dependent simulations. It starts from the left corner of the triangle in the $p - c$ diagram and ends on the opposite side. The densities of prey, predators and empty sites change continuously at $c(p)$. For $a \neq 0$, the transition is from the active state to the prey absorbing state. In the limiting case corresponding to $a = 0$, the point where $c(p)$ meets the right side of triangle of figure 1, the transition is from one of the infinitely many absorbing states to the prey absorbing state. For sets of parameters such that a approaches zero, the critical behaviour of the model suggests a crossover to another universality class. These features will be explored in section 3.

### 2.4. Growing clusters of predator–prey coexistence

The pictures shown in figures 4–6 are related to configurations generated by simulations of the predator–prey cellular automaton departing from the initial condition with one predator at the
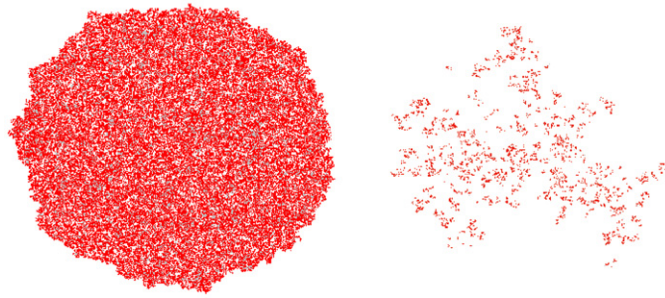
Figure 4. Two snapshots of the predator–prey automaton, generated from a single predator at the origin (centre) of a lattice covered by prey, for $p = -0.45$ and $c = 0.01$ (left panel, taken at $t = 10000$) and $c = 0.0227$ (right panel, taken at $t = 65000$). The white points represent sites occupied by prey, the black points (red points in the electronic version) by predators and the grey points are empty sites.
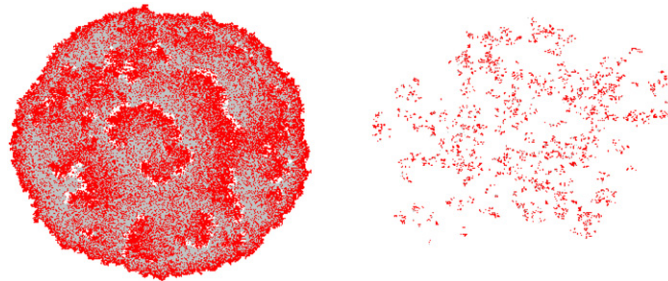

Figure 5. The same of figure 4, for $p = -0.3$ and $c = 0.0075$ (left panel, taken at $t = 1750$), and $c = 0.0867$ (right panel, taken after $t = 20000$).
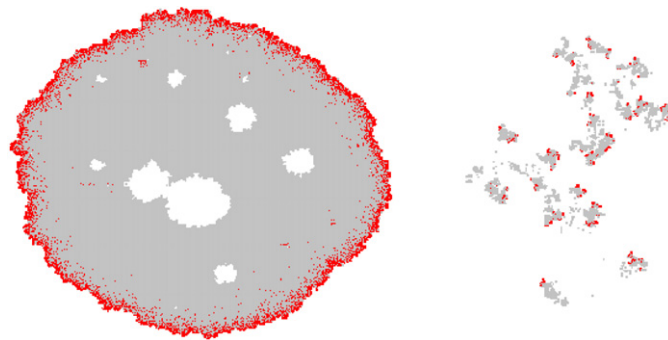
Figure 6. The same of figure 4, for $p = 0.3$ and $c = 0.06$ (left panel, taken at $t = 500$), and $c = 0.2257$ (right panel, taken at $t = 3000$).

origin and the lattice full of prey. It can be seen in figure 4 a configuration in the supercritical regime (left panel) and an almost critical configuration (right panel) for a set of parameters which corresponds to $b \ll a$ and $c \ll a$ (left down corner of the triangular phase diagram of figure 1). In this case, predators stay in the lattice for a long period of time, and when one of
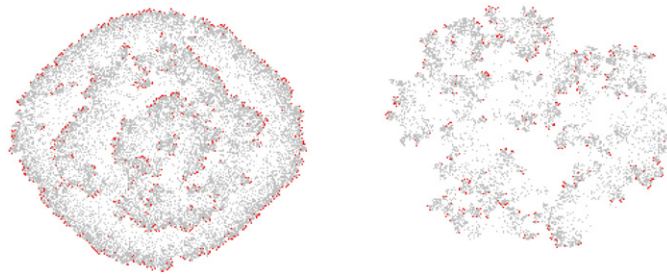
Figure 7. Two snapshots of the forest-fire model with immune trees, generated from a single burning tree at the origin (centre) of a lattice covered by green trees, for $p = 0.05$ and $g = 0.3$ (left panel, taken at $t = 200$) and $g = 0.45$ (right panel, taken at $t = 300$). The white points represent sites occupied by green tree, the black points (red points in the electronic version) by a burning tree and the grey points are empty sites.

them dies it gives place to an empty site that will be almost immediately occupied by a prey individual. Consequently, just a few number of empty sites is present in the steady state and also in the growing clusters. This behaviour suggests that the present three state process, in the limit $b \to 0$, $c \to 0$ with b/c finite, can be replaced by a two state process, similar to the contact process, involving predators and prey.

The growing cluster of the left panel of figure 5 shows a pattern formation related to an active region where prey and predators coexist and can exhibit local time coupled oscillations. With a nonzero probability, the dynamics will survive forever with the densities of each species different from zero but less than 1. Our numerical results indicate that this cluster, as well as the supercritical growing clusters of figures 4 and 6 (left panels), assumes after some characteristic time an asymptotic shape. At the critical point, this characteristic time diverges.

It is remarkable that the supercritical cluster of figure 6 corresponds to a configuration where the populations of prey and predators, under conditions of low densities, are grouped into small clusters of a unique species that are isolated from each other, and coexist without extinction in a highly heterogeneous space. In this respect, this species coexistence can be compared to the Huffaker's experiment, commented in section 1. The coexistence for the set of parameters of figure 6 is associated with self-sustained coupled time oscillations of prey and predators populations. These are local oscillations which have been detected by numerical simulations performed in finite size lattices [39].

Typical clusters at criticality are shown in the right panels of figures 4–6. According to our results of section 2.3, these configurations must be related with transitions belonging to the universality class of directed percolation. They present a shape of a fractal nature. We note that the critical cluster of figure 6 (right panel), which corresponds to a set of parameters inside the crossover region, presents, in contrast with those of figures 4 and 5 (right panels), noticeable agglomerations of empty sites. A qualitative similar behaviour of critical clusters was obtained by Dammer and Hinrichsen [35] for an epidemic spreading model which also presents a crossover from the directed percolation critical behaviour to the dynamic percolation critical behaviour.

We remark that the clusters present some characteristics in common with the clusters generated by the forest-fire model with immunization [37]. We have performed time-dependent simulations for this model, defined in a regular square lattice, considering the tree growth parameter $p = 0.05$ and immunity parameter $g = 0.3$ and $g = 0.45$. Snapshots are shown in figure 7 which should be compared with those of the predator–prey model shown in figure 5 if we interpret predators as burning trees and prey as green trees.

We finally should mention that simulations in finite systems, for some sets of parameters of the predator–prey automaton, may spuriously drive the system to be trapped either in an absorbing state where both species become extinct or in a prey absorbing state. These events occur especially for small values of c and/or in the crossover region; as explained by de Carvalho and Tomé [39], one method to determine whether in the stationary regime this state is attained, or not, is to avoid the extinction of species in the transient regime.

3. Spreading of an epidemic

3.1. The model

For $a = 0$ the predator–prey probabilistic cellular automaton can be interpreted as a model for the propagation of an epidemic with immunization. It mimics the spreading of an epidemic in a population composed of susceptible individuals (X) that get infected (Y) by contact with infected individuals; once infected the individuals can recover, and become immune (Z) spontaneously. The process of infection can be represented by the reaction

$$X + Y \rightarrow 2Y, \tag{11}$$

and the recovery process, which includes immunization, by the reaction

$$Y \rightarrow Z. \tag{12}$$

These are the basic processes which are taken into account in the modelling of the spreading of an epidemics with immunization [15, 20, 21, 31, 34, 35]. The present model is defined on a regular square lattice where each site can be in the following states: occupied by a susceptible, an infected or an immune individual. It comprehends the following stochastic rules.

(A) The infection can occur when a susceptible individual, which occupies a given site, has at least one site occupied by an infected individual in its neighbourhood, reaction (11). This process occurs with probability $b/4$ times the number of infected individuals in the neighbouring sites.
(B) The recovering process can occur spontaneously with probability c when a site is occupied by an infected individual, reaction (12). The condition $b + c = 1$ is obeyed, with b being the infection probability and c the recovery probability. This model can exhibit infinitely many absorbing states and presents a continuous transition belonging to the dynamic percolation universality class, as we show in section 3.3.
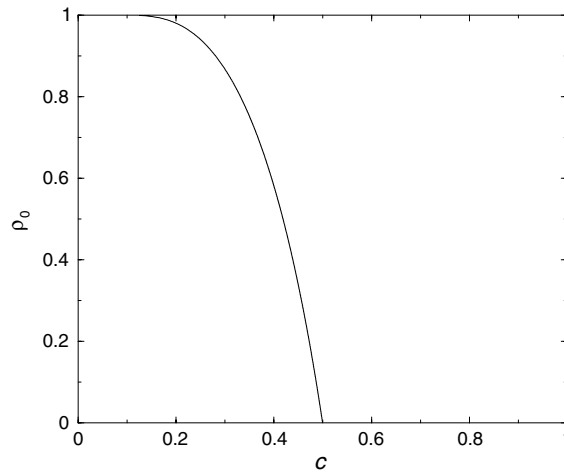
3.2. Mean-field approximation

The simplest mean-field approach for the epidemic spreading process is given from equations (4) and (5), with $a = 0$. So that

$$x_{\ell+1} = -b x_\ell y_\ell + x_\ell, \tag{13}$$

$$y_{l+1} = b x_\ell y_\ell + (1 - c) y_\ell, \tag{14}$$

where x_ℓ and y_ℓ are the densities of susceptible and infected individuals, respectively. The density of immune individuals is given by $z_\ell = 1 - x_\ell - y_\ell$. The stationary solution of this set of independent equations is such that $y = 0$ so that $x + z = 1$. To find the asymptotic values of x_ℓ for large values of ℓ we write down the following equation:

$$\frac{y_{\ell+1} - y_\ell}{x_{\ell+1} - x_\ell} = -1 + \frac{c}{b x_\ell}, \tag{15}$$

Figure 8. Density of immune individuals ρ_0 as a function of c, for $a = 0$, from mean-field approximation.

obtained from equations (13) and (14). For large values of ℓ, the left-hand side approaches the derivative $\mathrm{d}y/\mathrm{d}x$ so that

$$\frac{\mathrm{d}y}{\mathrm{d}x} = -1 + \frac{c}{bx}, \tag{16}$$

whose solution is

$$y = -x + \frac{c}{b}\ln x + 1. \tag{17}$$

The integration constant was found by considering that initially the individuals are all susceptible. In the stationary state $y = 0$ so that the asymptotic value of x is the solution of

$$-x + \frac{c}{b}\ln x + 1 = 0. \tag{18}$$

This equation was solved numerically and the result for $\rho_0 = z = 1 - x$ is plotted in figure 8. We can see that for small values of c the infection propagates over the susceptible population leaving a nonzero density of immune individuals. As c is increased a continuous phase transition to an absorbing state, where there is no spreading of the epidemic, takes place.

3.3. Time-dependent simulation

The spatial patterns and the threshold of the epidemic spreading can be obtained by performing time-dependent simulations. Initially all sites of the lattice are occupied by susceptible individuals except one, in the origin (centre) of the lattice, which is occupied by an infected individual. The stochastic dynamics follows the rules (A) and (B) defined in section 3.1 with a synchronous updating. The infection starts to be transmitted at time $t = 0$. We have performed an analysis similar to that shown in section 2.3 and investigated the time behaviour of the mean number of infected individuals $\langle N \rangle$, the survival probability P, and the mean-square distance of spreading from the origin $\langle R^2 \rangle$. The log–log plots of these quantities at criticality show a clear power-law behaviour, associated with critical behaviour, and the dynamic critical exponents η, δ and z, defined in the relations of equations (9), can be obtained. The estimated exponents are $\eta = 0.587(13)$, $\delta = 0.096(10)$ and $z = 1.767(5)$. The critical exponent $\nu_\parallel$ was obtained
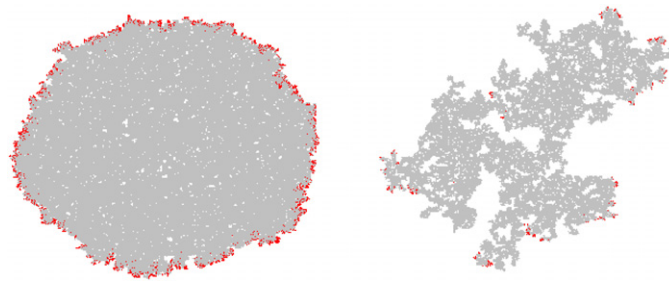
Figure 9. Two snapshots of the epidemic with immunization ($a = 0$) generated from a single infected individual located at the origin (centre) of a lattice covered by susceptible individuals, for $c = 0.15$ (left panel, taken at $t = 500$) and for $c = 0.22$ (right panel, taken at $t = 1000$). The white, black (red in the electronic version) and grey points represent sites occupied by susceptible, infected and immune individuals, respectively.

by analysing the behaviour of the derivative D, defined in equation (10), at the critical point. We have obtained the estimation $\nu_\parallel = 1.51(1)$. These exponents are consistent with the critical exponents of the dynamic percolation universality class [29] and this is the expected critical universal behaviour for a general epidemic with immunization [20, 21].

3.4. Patterns of spreading

For high values of the probability b of infection compared to the values of the recovering probability c, the epidemic spreads leaving a cluster of inactive sites composed of immune individuals and some groups of individuals which remain susceptible forever. A typical picture of the lattice in this situation is shown in the left panel of figure 9. The cluster grows with a front of infected individuals which stay in the border. After a finite time the cluster seems to assume a limiting shape and spreads to infinity with a nonzero probability. We observe that different initial seeds lead to different configurations of the spreading of the epidemic, giving rise to an infinitely many absorbing states. As b is decreased (and c is increased) the threshold for the spreading of the epidemics is reached. Above the threshold, the epidemic will cease in a finite time leaving a cluster with just a few number of immune individuals, the rest of the lattice being covered by susceptible individuals. A picture of the lattice near the threshold of epidemic spreading is shown in the right panel of figure 9. This almost critical cluster presents an irregular shape of fractal nature.

Similar critical and supercritical clusters have been obtained from time-dependent simulations for other spatial-structured stochastic models for an epidemic with immunization [27, 35] and for a forest-fire [43] model.

3.5. Steady-state simulation

We have considered square lattices with linear size L and periodic boundary conditions. For each value of L we have performed several independent simulations runs all starting from a lattice covered with susceptible individuals with the exception of one infected at the centre of the lattice. The system evolves in time according to the synchronous stochastic dynamics defined in section 3.1. In principle, any one of the infinitely many absorbing states can be reached; and, consequently, the number of immune individuals at the steady state varies from sample to sample. A simulation is finished when the system enters in an absorbing state and then the number of immune individuals is calculated. The mean value of this quantity, divided
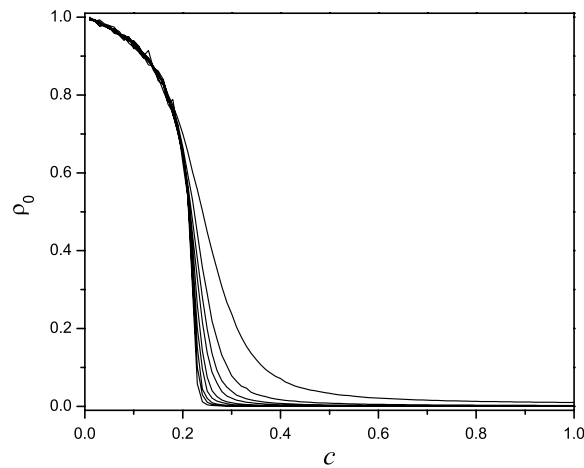
Figure 10. Density of immune individuals ρ_0 as a function of c, for $a = 0.0$. From top to bottom (at right): $L = 10, 20, 30, 40, 60, 80, 120, 160, 240$. The critical value of c for the infinite system is $c_c = 0.2200(3)$ (see table 1).
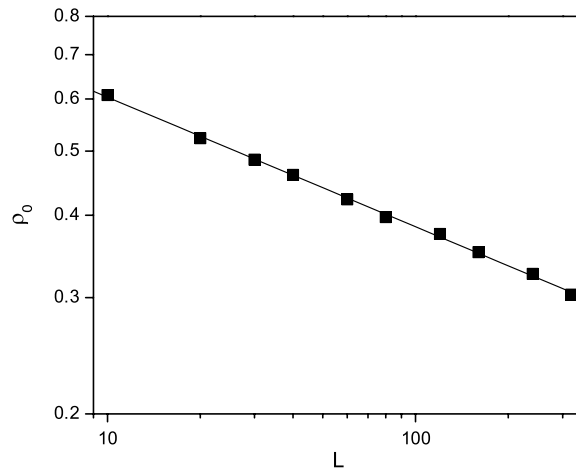
Figure 11. Log–log plot of ρ_0, calculated at the critical value $c_c = 0.220$, for $a = 0.0$, as a function of L. Simulations were performed on square lattices of size ranging from $L = 10$ until 320, and considering periodic boundary conditions.

by the total number of lattice sites L^2, is the density ρ_0 of immune individuals at the steady state (for a given lattice size).

The behaviour of ρ_0 as a function of c, for different values of L is shown in figure 10. In the subcritical regime (c above its critical value c_c) ρ_0 decreases as L is increased and in the limit $L \to \infty$ it vanishes. In the supercritical regime ρ_0 is almost independent of L. We have assumed that ρ_0 is an appropriate order parameter for this transition. For large values of L and off criticality the behaviour of ρ_0 versus c, shown in figure 10, is similar to that obtained from mean-field approximations (see figure 8).

Assuming the finite size scaling hypothesis [28] we expect that $\rho_0(\Delta, L)$, where $\Delta = c - c_c$, calculated for each value of L, scales at the critical point as, $\rho_0(0, L) \sim L^{-\beta/\nu_\perp}$, where $\nu_\perp$ is the critical exponent related to the spatial correlation length. To obtain the ratio $\beta/\nu_\perp$ we plot $\log \rho_0$, calculated at $c_c = 0.2200(3)$, versus $\log L$, as shown in figure 11. We

obtain $\beta/\nu_\perp = 0.185(5)$. Using the result $\nu_\perp = 4/3$ [29] we find the value $\beta = 0.139(4)$ which is in agreement with the one for the isotropic percolation, namely $\beta = 5/36$.

4. Summary

We have studied a spatial-structured model in which prey and predators individuals reside on the sites of a lattice and are described by discrete dynamic variables. The system evolves in time according to a probabilistic cellular automaton which takes into account the Lotka–Volterra interactions by the use of Markovian local rules. The model exhibits an active phase where prey and predator coexist without extinction, an absorbing prey phase, and, when the birth probability of prey vanishes, a phase with infinitely many absorbing states composed of empty (immune) sites and prey (susceptible). In the last case, it is more appropriate to refer to the predator–prey cellular automaton as a model for the spreading of an epidemic with immunization in a population composed of susceptible, infected and immune individuals. The automaton was studied by dynamic mean-field approximation and by numerical simulations which allow us to determine the phase boundaries (thresholds) and the critical exponents. We have localized a transition line that crosses the entire phase diagram. For all sets of parameters such that the prey birth probability is different from zero, this line separates the active phase, where prey and predators coexist, and the prey absorbing phase. We have shown that this transition belongs to the directed percolation universality class. We have also shown that when the prey birth probability equals zero, there is a crossover to the universality class of the dynamic percolation.

Patterns of growing clusters with coexistence of prey, predators and empty sites (or, susceptible, infected and immune individuals), generated by the time-dependent simulations, in the critical and in the supercritical regimes, were shown and discussed. The present study provides a detailed description of the thresholds of stable coexistence of the two species (or, the spreading of an epidemics) in the context of this predator–prey cellular automaton. We remark that the present model is one of the simplest spatial-structured models which contains the basic ingredients to describe the coexistence of two competing species and local oscillations. Once the phase diagram was achieved, other important ecological issues can be investigated. For example, the relevance of dispersion and explicit movement of individuals in determining the coexistence of species or the spreading of an epidemic. We expect that the introduction of these features, in the present stochastic space-structured model, should provide qualitative theoretical results that can be more realistic.

References

[1] Huffaker C B 1958 *Hilgardia* **27** 343
[2] Durrett R and Levin S 1994 *Theor. Popul. Biol.* **46** 363
[3] Tainaka K 1989 *Phys. Rev. Lett.* **63** 2688
[4] Satulovsky J and Tomé T 1994 *Phys. Rev.* E **49** 5073
[5] Boccara N, Roblin O and Roger M 1994 *Phys. Rev.* E **50** 4531
[6] Provata A, Nicolis G and Baras F 1999 *J. Chem. Phys.* **110** 8361
[7] Antal T and Droz M 2001 *Phys. Rev.* E **63** 056119
[8] Antal T, Droz M, Lipowsky A and Odor G 2001 *Phys. Rev.* E **64** 036118
[9] Ovaskainen O, Sato K, Bascompe J and Hanski I 2002 *J. Theor. Biol.* **215** 95

[10] Aguiar M A M, Rauch E M and Bar-Yam Y 2003 *Phys. Rev.* E **67** 047102
[11] de Carvalho K C and Tomé T 2004 *Mod. Phys. Lett.* B **18** 873
[12] Szabó G and Sznaider G A 2004 *Phys. Rev.* E **69** 031911
[13] Mobilia M, Georgiev I T and Täuber U C 2006 *Phys. Rev.* E **73** 040903
[14] Liggett T M 1985 *Interacting Particle Systems* (New York: Springer)
[15] Hastings A 1997 *Population Biology: Concepts and Models* (New York: Springer)
[16] Hanski I and Gilpin M E (ed) 1997 *Metapopulation Bilogy* (San Diego: Academic)
[17] Lotka A 1920 *J. Am. Chem. Soc.* **42** 1595
[18] Volterra V 1931 *Leçons sur la Théorie Mathématique de la Lutte pour la Vie* (Paris: Gauthier-Villars)
[19] Grassberger P and de la Torre A 1979 *Ann. Phys.* **122** 373
[20] Grassberger P 1983 *Math. Biosci.* **63** 157
[21] Cardy J L and Grassberger P 1985 *J. Phys. A: Math. Gen.* **18** L267
[22] Grassberger P 1989 *J. Phys. A: Math. Gen.* **22** 3673
[23] Grassberger P and Zhang Y-C 1996 *Physica* A **224** 189
[24] Jensen I, Fogedby H C and Dickman R 1990 *Phys. Rev.* A **41** 3411
[25] Dickman R and Tomé T 1991 *Phys. Rev.* A **44** 4833
[26] Jensen I 1992 *Phys. Rev.* A **45** 563
[27] Hinrichsen H 2000 *Adv. Phys.* **49** 815
[28] Marro J and Dickman R 1999 *Nonequilibrium Phase Transitions* (Cambridge: Cambridge University Press)
[29] Muñoz M A, Dickman R, Vespignani A and Zapperi S 1999 *Phys. Rev.* E **59** 6175
[30] Ódor G 2004 *Rev. Mod. Phys.* **76** 663
[31] Hinrichsen H 2006 *Physica* A **369** 1
[32] da Silva R, Dickman R and Drugowich de Felício J R 2004 *Phys. Rev.* E **70** 067701
[33] Arashiro E and Drugowich de Felício J R 2000 *Braz. J. Phys.* **30** 677
[34] Boccara N and Cheong K Y 1993 *J. Phys. A: Math. Gen.* **27** 1585
[35] Dammer S M and Hinrichsen H 2003 *Phys. Rev.* E **68** 016114
[36] Renshaw E 1991 *Modeling Bilogical Populations in Space and Time* (Cambridge: Cambridge University Press)
[37] Drossel B and Schwabl F 1993 *Physica* A **199** 183
[38] Tomé T 1994 *Physica* A **212** 99
[39] de Carvalho K C and Tomé T 2006 *Int. J. Mod. Phys.* C **17** 1647
[40] Domany E and Kinzel W 1984 *Phys. Rev. Lett.* **53** 447
[41] Grassberger P 1995 *J. Stat. Phys.* **79** 13
[42] Ziff R, Gulari E and Barshad Y 1986 *Phys. Rev. Lett.* **56** 2553
[43] Albano E 1995 *Physica* A **216** 213